Journal of Muscle Research and Cell Motility **22**: 635–646, 2001.

Fluorescence changes on contractile activation in TnC_{DANZ} labeled skinned rabbit psoas fibers

MICHAEL HUANG[1], DANIEL BURKHOFF[2], FRED SCHACHAT[3] and PHILIP W. BRANDT[4,*]
Departments of [1]Biomedical Engineering, [2]Medicine, Columbia University; [3]Department of Cell Biology, Duke University; [4]Department of Anatomy and Cell Biology, Columbia University, 630 West 168 St., New York, NY 10032, USA

Received 3 April 2001; accepted in revised form 6 November 2001

Abstract

The increase in fluorescence of dansylaziridine (DANZ) labeled troponin C (TnC_{DANZ}) substituted into skinned rabbit psoas fibers was determined as a function of the pCa. The fluorescence data are expressed as the ratio of two wavelength bands, one that sees the fluorescence of TnC_{DANZ}, and one that sees background fluorescence and scatter. The percent TnC replaced with TnC_{DANZ} was varied between 10 and 50% and, the fibers were randomly stretched, at the start of each experiment, between 10 and 50%. A large ratio increase accompanies increase in $[Ca^{2+}]$. The pCa/force data are best fit by the Hill equation but the pCa/ratio data are best fit by a model in which Ca^{2+} binds in two phases. The position of the force curve on the pCa axis varies little between fibers, in contrast to that of the ratio or Δ-fluorescence curve. In accord with previous reports the Δ-fluorescence can be left of the force on the pCa axis (type I) or superimpose in part on the force (type II). Not described previously, we find curves in which the second phase of the ratio cross-over the pCa/force curve. This type III relationship is found only in fibers less than 3 weeks postmuscle harvest. We propose that the first, relatively invariant, phase of the biphasic pCa/ratio curve accompanies Ca^{2+} binding to either of the two low affinity sites on TnC_{DANZ} as it does for TnC in solution. The second, highly cooperative, phase of the ratio curve that accompanies muscle contraction and enhanced Ca^{2+} binding is initiated when sufficient Ca^{2+} is bound to overcome inhibitory systems. Loose coupling between the initial Ca^{2+} binding and the cooperative switch point may account for much of the variation in the shape and position of the pCa/ratio curve. There is evidence that, in the overlap zone, weakly attached myosin cross-bridges enhance cooperation between the regulatory units of the thin filaments.

Introduction

Skinned fibers bathed in low $[Ca^{2+}]$ solutions (pCa 8) containing millimolar substrate (MgATP) are relaxed; as the pCa is reduced, ($[Ca^{2+}]$ increased) force develops at about pCa 6 and saturates by 5.5. When troponin C (TnC) is extracted from isolated myofibrils (Zot and Potter 1982) or skinned fibers they no longer respond to high $[Ca^{2+}]$ (Brandt *et al.*, 1984a,b, 1987; Moss *et al.*, 1985). From these and many other experiments (Weber and Winicur, 1961; Ebashi *et al.*, 1969; Potter and Gergely, 1975) it is apparent that Ca^{2+} binding to TnC triggers muscle contraction. The exact relationship, however, between force development and Ca^{2+} binding is uncertain.

When Ca^{2+} binding to myofibrils is directly measured by isotope methods the amount of Ca^{2+} bound parallels (Fuchs, 1985) or perhaps slightly precedes the pCa/force curve (Fuchs and Fox, 1982). When Ca^{2+} binding to TnC in solution is measured by fluorescence change in DANZ attached to methionine 25 (Johnson *et al.*, 1978), binding to either of the two low affinity regulatory sites doubles fluorescence while binding to both sites does not further increase fluorescence. Binding to the two high affinity structural sites reduces fluorescence by 20%. The development of a technique to specifically extract and replace the TnC of skinned muscle fibers (Brandt *et al.*, 1984 a,b; Moss *et al.*, 1985) allowed the relationship between Ca^{2+} binding and force to be studied in single skinned muscles in which TnC_{DANZ} replaced native TnC (Guth and Potter, 1987; Morano and Ruegg, 1991; Zot and Potter 1987). In TnC_{DANZ} substituted fibers the pCa/Ca^{2+}-binding curve did not superimpose on the pCa/force curve but was parallel and 0.6 pCa units higher. A similar study by Allen *et al.* (1992) found the pCa/Δ-fluorescence curve to be biphasic; one phase preceded force and a second phase superimposed on the upper part of the pCa/force curve. The authors argue that the first phase results from Ca^{2+} binding to the high affinity TnC_{DANZ} sites and the second from Ca^{2+} binding to the low affinity, regulatory sites.

There are complex interactions in the myofilament system that may also influence TnC structure and thus the fluorescence of TnC_{DANZ}. Fuchs (1977) reports that

* To whom correspondence should be addressed: E-mail: pwb3@columbia.edu

rigor cross-bridges enhance Ca^{2+} binding to myofibrils. The fluorescence of TnC_{DANZ} is reported to be increased by rigor cross-bridges as much or more so than by Ca^{2+} binding (Guth and Potter, 1987; Morano and Ruegg, 1991; Allen *et al*., 1992). A study following dichrosim of 5'ATR on Cys98 of TnC in skinned fibers also finds that rigor cross-bridges affect the conformation of TnC although less strongly than Ca^{2+} binding (Martyn *et al*., 1999).

The pCa/force relationship of rabbit psoas fibers is steep with Hill coefficients (n_H) of 5 or more (Brandt *et al*., 1980; Moss *et al*., 1983), greater than can be explained by Ca^{2+} binding, cooperative or otherwise, to the two regulatory sites on a single TnC (Brandt *et al*., 1980). Several mechanisms have been suggested to contribute to the large n_Hs. One proposal is that one or more cycling cross-bridge states enhance thin filament activation, a form of positive feedback (Moss, 1992; Gordon *et al*., 2000). Based on the extreme sensitivity of the n_H to partial TnC extraction, we suggested that all regulatory units (one troponin, one tropomyosin and seven actins) of the regulatory strand (26 units) interact cooperatively (Brandt *et al*., 1984b, 1987; Fraser and Marston 1995). Because of cooperative interactions between regulatory units, the Ca^{2+} affinity of all the TnCs of a strand increases in concert when the thin filament switches from the relaxed to the active configuration (Brandt *et al*., 1987).

In the present study of the cooperative relationship between the pCa/force, Ca^{2+} binding, and cross-bridge states, we extracted various amounts of TnC from skinned rabbit psoas fibers and replaced it with TnC_{DANZ}. To determine the degree to which active cross-bridges contribute to the fluorescence increase of TnC_{DANZ} we varied their numbers by randomly stretching fibers between 10 and 50% of slack length. We also reduced the number of force cross-bridges by bathing fibers in 1 mM vanadate. TnC is more rapidly extracted from the I-band than from the overlap zone or A-I-band (Swartz *et al*., 1997; Yates *et al*., 1993) and this could result in more TnC_{DANZ} in the I-band than in the A-I-band. In addition, the pCa/Δ-fluorescence signal may vary with the location of the TnC_{DANZ}. To see if TnC_{DANZ} in the I-band produces a different signal that that in the overlap band a correlation was sought between the TnC_{DANZ} signal and percent fiber stretch. Furthermore, in some experiments the TnC in the I band was extracted prior to collection of pCa/Δ-fluorescence data. To determine if the pCa/TnC_{DANZ} fluorescence varies with the amount of TnC replaced, a range of replacement between 10 and 50% was tested; with low replacement amounts a greater proportion of the TnC_{DANZ} would end up in the I-band and with 50% replacement most would be in the A-I-band. To define as precisely as possible the slopes, shapes and relative positions of the pCa/force and pCa/Δ-fluorescence curves in TnC_{DANZ} substituted fibers and to minimize artifacts from fiber movement and shape change that accompany contraction, two separate fluorescence wavelength bands are monitored, one for TnC_{DANZ} and one to assay the amount of fiber in the aperture. The ratio of these two bands reports a more reliable Δ-fluorescence than the single wavelength method. To minimize TnC_{DANZ} bleaching a stable form of flash illumination is employed.

Methods

Muscle preparation

A New Zealand white rabbit is euthanized and strips of psoas muscle 1–2 mm in diameter and 50 mm in length are separated longitudinally from the whole muscle and tied to small wooden sticks in three places about 1.5 cm apart. The ends of the strips are then cut free of the muscle and, to destroy the surface membranes, the strips immersed in a skinning solution at 0°C for 24 h. The Skinning solution contains 5 mM EGTA, 2.5 mM MgATP, 170 mM potassium propionate, and 10 mM imidazole at pH 7.00 (Wood *et al*., 1975; Eastwood *et al*., 1979).

After the muscle is skinned, it is placed in a glycerol–saline 'Storage solution' at 0°C for one day then for long term storage transferred to a −20°C freezer. Storage solution consists of 170 mM potassium propionate, 2.5 mM MgATP, 10 mM imidazole, 5 mM EGTA, and 50% (by volume) glycerol. Both solutions are changed several times. Groups of about 50 fibers are pulled from the main bundle then single fibers are dissected in cold storage solution. The average fiber length (between hooks) and diameter is about 5 mm and 80 μm, respectively. All forces are in milligrams per fiber.

Apparatus

The apparatus is constructed around an inverted microscope to enable the simultaneous measurement of change in fluorescence of TnC_{DANZ}, background fluorescence, and force in single skinned muscle fibers. The muscle chamber (Brandt *et al*., 1980) is mounted on the stage of a Nikon Inverted epifluorescence microscope (Nikon Diaphot-TMD-EF) equipped with a 20X objective (0.75 N.A.). Ultraviolet (UV) light passing through the objective excites the TnC_{DANZ} probe in the muscle and the emitted light passes back through the objective then through an array of filters to photomultipliers. Approximately 0.5 mm of fiber length is in the photomultiplier system aperture. The photomultipliers are output to an A/D converter in a computer that controls the apparatus, the experiment protocol and data acquisition.

After a single fiber is dissected and labeled with TnC_{DANZ}, it is attached to stainless steel hooks inside the chamber and randomly stretched between 10 and 50% of slack length. One hook extends to a strain gauge to measure force and the other to a screw to set fiber length. Beginning with pCa 8.0 'relaxing solution', in the

chamber precision pumps (Valcor Engineering Corp.; Springfield, NJ; models 550A197-2 and 525A197-2) are commanded to change the bathing solution or to incrementally add small aliquots of another solution. A vibrating stainless steel tube both stirs, and on computer command, skims fluid from the top of the solution to keep the volume constant. The pump for pCa 4.75 delivers 10 μl increments with each impulse to step the initial pCa 8 in the chamber to higher [Ca^{2+}] (Brandt *et al*., 1980). At stable force after each step, fluorescence and force are recorded. The fibers begin to contract at about pCa 6.0 and force saturates by pCa 5.5. With this 'serial dilution method' the steady state force and fluorescence is determined at each step change in pCa between approximately 8 and 5 (Brandt *et al*., 1980). Temperature regulated water is pumped through channels in the chamber walls and to a small water bath next to the chamber where the stock pCa 8 and pCa 4.75 solutions are kept. The chamber and the solutions are held at 20°C.

Force transducer

This has been described previously (Brandt *et al*., 1980). The filtered output is sent to an A/D converter channel in the computer. Force is sampled at each interrupt (810/s) and averaged over one second.

Labeling troponin C

DANZ labeling of TnC followed procedures similar to those of Johnson *et al*. (1978). Rabbit skeletal TnC is grown in bacteria through expression of the pET17 vector system (Novagen). After purification a solution of 2 mg/ml skeletal TnC in 10 mM potassium phosphate, 90 mM KCl, 2.5 mM $CaCl_2$ and 2 mM EGTA (pH 7.0) is labeled by adding 0.01 M dansylaziridine (DANZ; Molecular Probes, Eugene, OR) dissolved in ethanol until it is 0.5 mM excess over TnC. The mixture of TnC and DANZ is incubated for 24 h in the dark at room temperature. Following incubation, the solution is dialyzed several times against 10 mM phosphate, 90 mM KCl, and 2 mM EGTA (pH 7.0). This produces TnC with DANZ bound to methionine 25, part of calcium-binding loop 2 (Johnson *et al*., 1978).

Substituting TnC_{DANZ} for intrinsic TnC

Four to six single fibers, approximately 20 mm in length, are isolated and transferred to a small plastic Petri dish of relaxing solution. The fibers are slightly stretched (about 10%) and the ends are fixed to the bottom of the dish with dabs of silicon rubber. The dish is drained and filled twice with 'Wash solution'(195 mM propionate, 10 mM morpholinopropane sulfonic acid, MOPS) to remove EGTA, MgATP, and ATP from the fiber then the Wash is replaced with pCa 8 'Rigor solution' (1.3 mM calcium propionate, 10 mM EDTA, 60 mM sodium propionate, 28.7 mM Na_2SO_4, pH 7.00). Finally, the Rigor solution is replaced with 'Extraction solution' (5 mM EDTA, 10 mM MOPS, pH 7.2 at 32°C) for 30 s to 2 min. The extraction solution is removed and the fibers are again immersed in relaxing solution. This protocol of wash, rigor, and extraction removes 10–50% of the native TnC (Brandt *et al*., 1984a,b, 1987). The extracted fibers are incubated in the dark at room temperature in 100 μg/ml of TnC_{DANZ} in pCa 8 solution for 20–30 min then washed in pCa 8 and stored at 4°C in the dark until used. Fresh fibers are prepared each day.

pCa solutions

Solutions are made from stocks following recipes printed by a program that inputs the desired final composition (Brandt *et al*., 1972, 1987). The ionic strength, monovalent cation concentration, MgATP, and total phosphate are constant throughout the experiments. Free ATP (0.47–5 mM) is used to buffer the MgATP. Two 'low Mg^{2+}' solutions at pMg 4.0 are: (1) pCa 8.0 (Relaxing solution) contains (in mM) 10 EGTA, 0.19 $CaPr_2$ (Pr = propionate), 0.1 $MgPr_2$, 5 free ATP, 5 MgATP, 7.5 PO_4, 80 NaPr, 0.81 Na_2SO_4, and 10 MOPS (morpholinopropane sulfonic acid). (2) pCa 4.75 contains 10 CaEGTA, 0.18 $CaPr_2$, 0.078 $MgPr_2$, 5 free ATP, 5 MgATP, 7.5 PO_4, 60 NaPr, 0.37 Na_2SO_4 and 10 MOPS (pH 7.0).

Two alternate 'high Mg^{2+}' solutions at pMg 3.0 are: (1) pCa 8.0 contains (in mM), 10 EGTA, 0.18 $CaPr_2$, 1.0 $MgPr_2$, 0.47 free ATP, 5 MgATP, 7.5 PO_4, 34 NaPr, 29.9 Na_2SO_4, and 10 MOPS. (2) pCa 4.75 contains 10 CaEGTA, 1 $MgPr_2$, 3 mM free ATP, 5 mM MgATP, 7.5 mM PO_4, 15 mM NaPr, 29.9 mM Na_2SO_4, and 10 mM MOPS.

Measuring fluorescence

UV light from a 75-watt xenon arc lamp (Photon Technology International, Inc.; Princeton, NJ) is directed to a mirror mounted on a wobbler. This oscillates at 405 Hz reflecting the UV light through approximately a 20° arc. The UV light reflected from the wobbler passes through a lens to fixed mirror that reflects UV light towards the aperture of the microscope. As the beam sweeps over the aperture of the fluorescence microscope the fiber is briefly illuminated. Just as the UV sweep starts across the aperture of the microscope, a strobe (810/sec) initiates integration and all the fluorescence emitted during the UV sweep is integrated into a single voltage that is read by the A/D converter. A/D converters have windows of capture of a few μsec; the integrators in effect expand this to cover the whole time the illumination sweep occupies the aperture to the microscope. A mechanical shutter blocks the UV light between data collections.

The excitation bandwidth is from 330 to 380 nm. A dichroic mirror reflects all wavelengths below 455 nm to

the muscle fiber and transmits all higher wavelengths to the photometer system. The transmitted or emission wavelengths from the fiber are separated at 580 nm with a second dichroic mirror into Red and Green channels. The bandwidth of the Green channel (TnC_{DANZ} emission) is from 510 to 560 nm and the bandwidth of the Red channel is from 610 up. Each channel is directed into a separate photomultiplier (Hamamatsu Corp.; Bridgewater, NJ). The photomultiplier outputs go to integrators that in turn output to separate A/D converter channels. Alternate sweeps are read from the Red or Green A/D channel.

An interrupt to the computer is generated by each sweep (two sweeps/cycle of the wobbler) causing the computer to jump to an assembly program running in the background. The assembly program directs the A/D converter, stores the data in memory, controls the pumps and valves to automate the experimental protocol. A basic program in the foreground sets up the assembly program's variables, displays the data as it is collected, stops/starts interrupts, and writes the data to disk files after completion of each protocol step. All the protocols are text files.

Fluorescence is in millivolts. At standard amplification background fluorescence (plus dark current) of a chamber filled with pCa 8 is about 10–20 mV. All the baseline fluorescence values given in the results include the background fluorescence. The anode voltages on the two photomultipliers are set so that output voltages are about the same for TnC_{DANZ} fibers in pCa 8. At least 90% of all the experiments were done with the Red channel photomultiplier anode set to 950 V and the Green to 825 V. Fluorescence is sampled for one second (405 readings/channel) at each pCa.

Data analysis

Force data are fit to the standard Hill equation yielding two fitting parameters pK_F and n_H, the midpoint and slope respectively of the pCa/force relationship (Brandt *et al.*, 1980). Fluorescence data are fit using Origin's scripting language (Microcal Software Inc; Northampton, MA) to a one-binding-site model (half of Equation 1) and to a two-site model (Equation 1).

$$Y = A/(1 + (10^{(\mathrm{pCa}-\mathrm{p}K_1)})^{n^1}) + (1-A)/(1 + (10^{(\mathrm{pCa}-\mathrm{p}K_2)})^{n^2}) \quad (1)$$

Equation 1 has five variable parameters: A, pK_1, pK_2, n_1, and n_2. The parameters, A and $1-A$ are the relative magnitudes that each site contributes to the total Δ-fluorescence. The parameters, pK_1 and pK_2, are the pCa_{50} values of each site. The parameters, n_1 and n_2, are the slopes of the curves. A simplified fitting uses three variable parameters pK_1, pK_2, and n_2 and two fixed parameters, $A = 0.5$, and $n_1 = 1$ that is approximately true for most experiments.

Results

Movement artifact and channel spillover

To reduce artifacts of fiber movement and changes in fiber density we constructed a dual wavelength apparatus. One channel, green, (see methods for wavelengths) monitors changes in fluorescence specific to TnC_{DANZ} and the other channel, red, monitors changes in the amount and/or geometry of the fiber image in the aperture of the photomultipliers. By forming the green: red ratio fiber movement artifacts are minimized. To show that this ratio compensates for muscle movement a fiber was gradually moved into the aperture of the photomultipliers (Figure 1).

As the fiber enters the aperture, (Arrow) both the red (○) and the green (□) channel fluorescence intensities progressively increase in parallel. Because TnC_{DANZ} greatly increases light in the green over the red channel the initial absolute, output voltage of each channel is adjusted to bring the ratio to near unity. The ratio (△) is very noisy when the fiber is out of the field then increases and becomes relatively stable as soon as the fiber partially enters the aperture of the photomultipliers even though the green and red channels are still rising. (For better resolution the ratio of Figure 1 is multiplied by 100.) Because the ratio is more stable than the green channel, the data presented here are expressed as the green:red ratio. Although the green channel can usually be substituted for the ratio with only small qualitative changes in the results, the red channel also provides

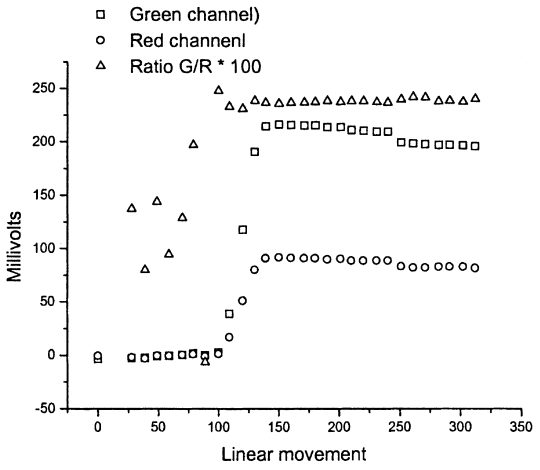

Fig. 1. This figure illustrates the effect of fiber movement on the ratio (△) of the green:red channels. The raw data are plotted against time as the fiber is gradually stepped into the aperture of the photomultipliers. When the edge of the fiber enters the aperture the fluorescence in the red (○) and green (□) channels starts to increase. Some fibers were treated with rhodamine labeled phalloidin to increase the red channel fluorescence but the benefit was small and did not improve the ratio or the discrimination of red channel drop off enough to risk potential side effects (Data not shown). In this experiment, the background fluorescence of each channel could be measured before the fiber entered the aperture and it was subtracted prior to the formation of the ratio. In the rest of the experiments reported here this was not possible.

independent evidence of fiber movement that can produce misleading green channel data.

Figure 2A is a plot of the normalized raw data against time. For the first 200 s 10 aliquots of pCa 8 are added to establish a baseline and, after a pause, incremental volumes of pCa 4.75 are added to generate a stepwise increase in $[Ca^{2+}]$. Force starts up at about 450 s as threshold $[Ca^{2+}]$ is reached. The green and red fluorescence and their ratio also increase with decreasing pCa, but not in parallel with force.

Some of the TnC_{DANZ} signal appears to enter the red channel. This is expected because the TnC_{DANZ} fluorescence is spectrally broad enough for some to enter the red window. The spillover of TnC_{DANZ} into the red channel can be removed by subtracting 25% of the green from the red channel. After subtraction, variation in the red channel is reduced to 2% of baseline (Figure 2B). This signifies that the fiber remained relatively stable in the aperture of the photomultipliers throughout the contraction. Examples where the corrected red channel signal is not random are described later. Although subtraction of 25% of the green from the red channel greatly changes the appearance of the normalized red channel, the ratio change is small (compare panels A and B).

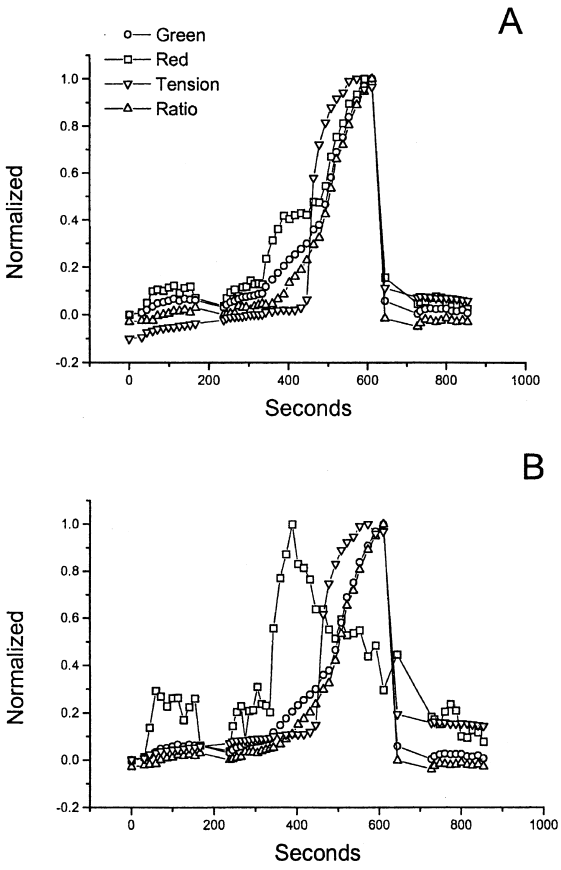

Fig. 2. (A) The normalized raw data collected during a pCa/force experiment is plotted against time. Each symbol in the figure is the steady reading following solution injection. First, pCa 8 is injected 11 times, then a 1-min pause, then pCa 4.75 is injected 28 times, next, the fiber is relaxed by replacing the solution in the chamber with pCa 8. Finally, pCa 8 is again injected 11 more times. The fluorescence of both the red (□) and the green (○) channels start rising at about 320 s and at about 440 s force (▽) abruptly rises. Base millivolts for green and red are 388 and 347 respectively and the Δ-fluorescence is 105 and 29 mV respectively. To set the green:red ratio near unity, the voltages on the photomultipliers are adjusted to 825 and 950 volts respectively. (B) The same data as in A but 25% of green is subtracted from red then base millivolts are added back. Red no longer follows green. Base millivolts for green and red are 384 and 341 respectively and the Δ-fluorescence is 108 and 6.8 mV respectively. The raw data are reduced and plotted with Origin's scripting language (Microcal Software Inc.; Northampton, MA).

After eliminating green spillover from the red channel, the remaining red signal (□) of panel B still measures light emitted by or scatter from the fiber. If the corrected red channel is relatively invariant throughout the experiment, we consider the data reliable. As a corollary, if there is drop off in the red channel (before or after subtraction of the green; drop off can only increase with subtraction.), fiber movement is the probable cause. Movement that causes systematic drop off in the red will also perturb the green channel although this may not be evident. Whenever there is drop off in the red channel of more than a few percent we discard the experiment.

An experiment is considered valid if there is no significant drop in the red channel. If the red drops it is likely that fiber movement, including stretching, has also reduced the Ca^{2+}-binding (green) signal. Two examples of drop off in the red channel are shown in Figure 3. In panels A and C the ratio curves plotted against the pCa are completely left of the force curves. In panel A there is a notch in the ratio before it peaks. This may indicate that the fiber moved or possibly stretched during the collection of data. The significance of the notch is clear in panel B, the plot of the raw data with time. The red channel drops steeply (with no subtraction of green spillover) starting at the notch in the ratio and falls almost to the baseline as force saturates. The green channel also falls but not as steeply. The ratio of the two channels has the notch but overall does not fall. In this case, the ratio compensates at least partially for the drop off in the two channels. A second example of drop off in the red channel raw data is shown in panel D. Although the ratio plot, panel C, is smooth and free of notches, there is a drop off in the red channel. If the fibers of Figure 3 had not moved it is possible that the saturation of the ratios would have been higher. Because the red channel drops off so much the data are not reliable. Of about 200 complete data sets, approximately half were discarded because the red channel dropped off during muscle contraction. None of the discarded curves is type III (see below); all have pCa/ratio curves left of the pCa/force curves. In almost all of the discarded experiments the ratios (and green channels) either dropped after an initial rise or reached a plateau well before the force curve saturated.

pCa/force/ratio

In Figure 4 the normalized green/red ratio and force data of Figure 2 are plotted against the pCa. The pCa/force

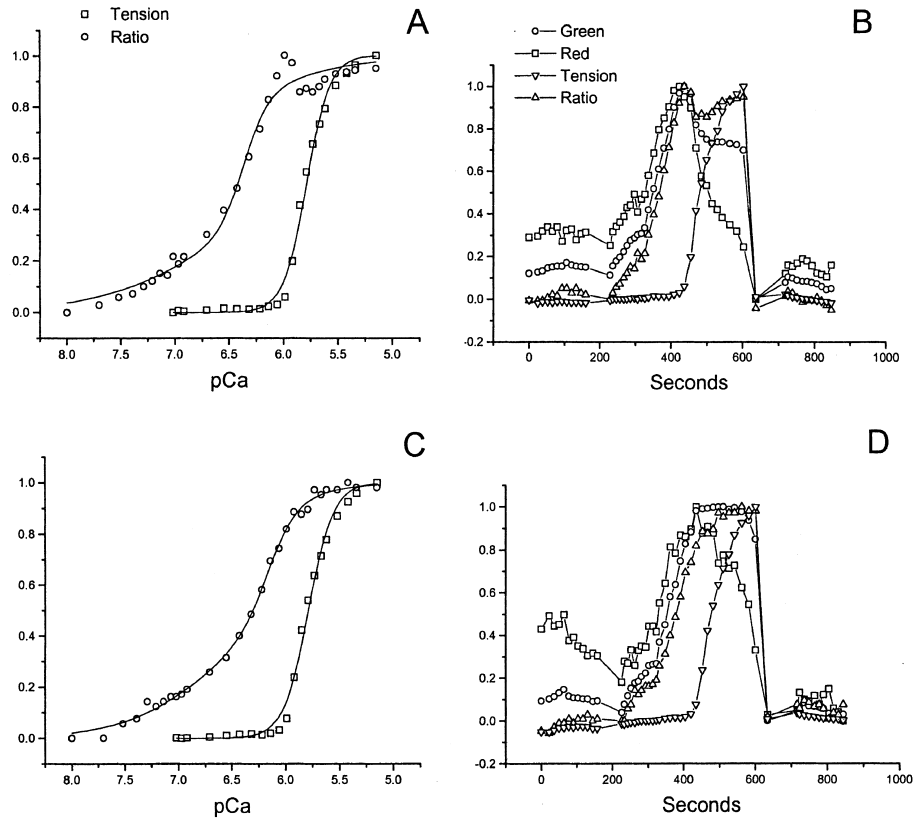

Fig. 3. The red channel can be used to identify possible movement artifacts. (A) pCa against normalized force and ratio. The notch in the ratio (○) near the top of the curve could be due to fiber movement. (B) The raw red ( ) and green (○) data for panel (A) show obvious drop offs. (C) A data set with no notch in the ratio even though (D) the red channel raw data dropped almost to the baseline and the green channel flattened then dropped. For (A) $pK_F = 5.79$, $n_H = 3.4$ and (B) $pK_1 = 6.68$, $pK_2 = 6.37$, $n_1 = 0.83$, $n_2 = 3.93$, $\chi^2 = 0.002$,. For (C) $pK_F = 5.79$, $n_H = 3.76$ and (D) $pK_1 = 6.73$, $pK_2 = 6.16$, $n_1 = 1.1$, $n_2 = 3.2$, $\chi^2 = 0.00035$. In (B) the base and Δ for the green channel are 351 and 52, and those for the red channel are 261 and 11. For (D) the base and Δ are, green 458 and 48, and red 365 and 12.

points are fit to the Hill equation and are identical in all three panels. The ratio data points are fit by a least squares method to one of three models and smooth curves are constructed from the fitted parameters. In panel A the ratio is fit to a model that sums two cooperative classes of binding sites. The fitting equation has five free parameters (Methods). The curve fits well to the ratio data points and the fitted parameters are listed in the Figure legend. The p*K*s of the two putative sites differ by 0.57 pCa units. In panel B the same data is fit with three free parameters, pK_1, pK_2 and n_2. The value of n_1 is fixed to 1 and it is assumed that the two sites contribute equally to the fluorescence change ($A = 0.5$). The data are fit about as well as with five free parameters (Compare χ^2 for panels A and B). These two sites separate by 0.83 pCa units. One-binding site is assumed in panel C with two free parameters, pK_1 and n_1 and most of the points at the foot of the curve are above the line. The χ^2 (2.0 E-3) is 10 times larger than that of panel A and five times larger than that of B. For the vast majority of data the two-binding site model, as in panel A, consistently produces a much better fit than the one site model.

The first part of the pCa/ratio curve in Figure 4 takes place before force appears, therefore, it is not subject to signal distortion from fiber movement. The second part of the ratio curve overlaps the rise of force and continues to rise after force saturates. Therefore, the normalized pCa/ratio curve crosses over the normalized pCa/force curve. This relation between the pCa/force and the pCa/ratio curves is called type III.

Two to three sequential data collections are made on most fibers. In general, the second pCa/ratio curve closely resembles the first but, the relation to the force curve changes subtly. This is because the pCa/force curve is usually a little lower in slope (and force) on repetition and this tends to reduce the degree of cross-over for type III curves. Stretching the fibers between 10 and 50% has no discernable affect on the frequency of type III curves.

Among the data sets accepted (no drop off in the red channel) are those where the ratio curves converge with force near the top (Type II curves); the ratio does not cross-over the force curve. An example of an experiment done in 1 mM Mg^{2+} is shown in Figure 5. The ratio data is fit well by the two-site model and five free parameters (panel A). The difference between the pK_1 and pK_2 is 0.85 pCa units. In panel B, the smooth curve drawn from fitting parameters from the one-site model

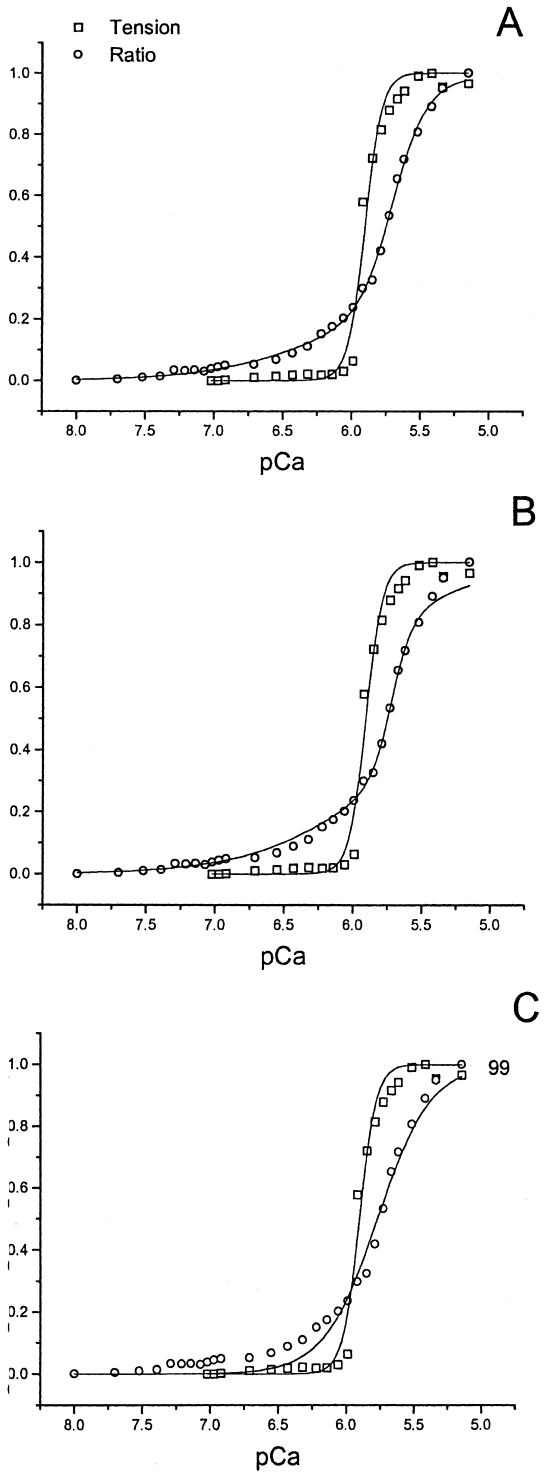

Fig. 4. (A) The normalized ratio (○) and force (□) data of Figure 2B plotted against the pCa. The ratio curve crosses over the force curve (type III relation). The ratio data are fit to the two calcium binding site model using five free parameters. The smooth curve is drawn with $pK_1 = 6.27$, $pK_2 = 5.70$, $n_1 = 1.07$, $n_2 = 3.56$, $A = 0.25$, and the $\chi^2 = 0.00021$. The force data are fit to the Hill equation and the smooth curve is drawn with $pK_F = 5.91$ and $n_H = 7.2$, $P_o = 99$ mg. (B) The same ratio and force data as in (A) but the ratio data are fit to the two site model with three free parameters. The value of n_1 is fixed at 1.0 and A is fixed at 0.5. The fitted parameters are $pK_1 = 5.91$, $pK_2 = 5.72$, $n_2 = 5.93$ and the $\chi^2 = 0.00054$. The fit is almost as good as (A). (C) The same ratio and force data as in (A) but the ratio data are fit with a one site model. The smooth curve is drawn from the best fit parameters, $pK_1 = 5.77$, $n_1 = 2.24$, and the $\chi^2 = 0.002$.

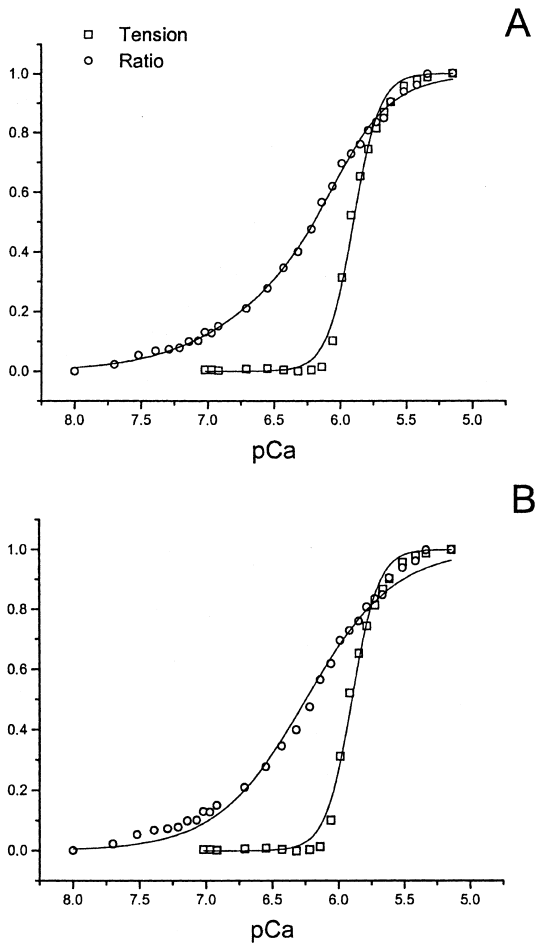

Fig. 5. (A) The pCa/ratio converges with the pCa/force near the top (Type II relationship) without crossing over as in Figure 4. For force the fitted parameters are $pK_F = 5.91$ and $n_H = 4.4$, $P_o = 75$ mg. The fitted ratio parameters are $pK_1 = 6.93$, $pK_2 = 6.08$, $n_1 = 1.2$, $n_2 = 1.2$, $A = 0.25$, and the $\chi^2 = 0.0002$. The smooth curves are drawn using these parameters. (B) The same force and ratio data are shown but the ratio data are fit with a model for one binding site. $pK_1 = 6.25$, $n_1 = 1.3$, and the $\chi^2 = 0.0009$. Data collected in 1.0 mM Mg^{2+}.

misses many points at the foot and top of the ratio curve. Comparing points on the smooth curve in panel A with those in B justifies the two-site model. This conclusion is further supported by comparison of the χ^2.

The data of Figure 6 were collected in 0.1 mM [Mg^{2+}]. The pCa/ratio curve is further left of the pCa/force curve that that of Figures 4 and 5, and it is called a type I curve. Again, two models are used to fit the ratio curves, and again χ^2 support the two binding-site over the one-site model. The difference between the pK_1 and pK_2 is about 0.4 pCa units. In almost all experiments, either in high or low [Mg^{2+}], the one site model fails especially to fit the data at the left end of the ratio curve. The relative positions of the force and ratio curves do not correlate with [Mg^{2+}] concentration. The mean pK_1s in high (1 mM) and low [Mg^{2+}] (0.1 mM) are about the same (6.215 and 6.291 respectively).

In Figures 4, 5 and 6 the relationship between the ratio and force curves is not the same. This is surprising because the underlying assumption is that the

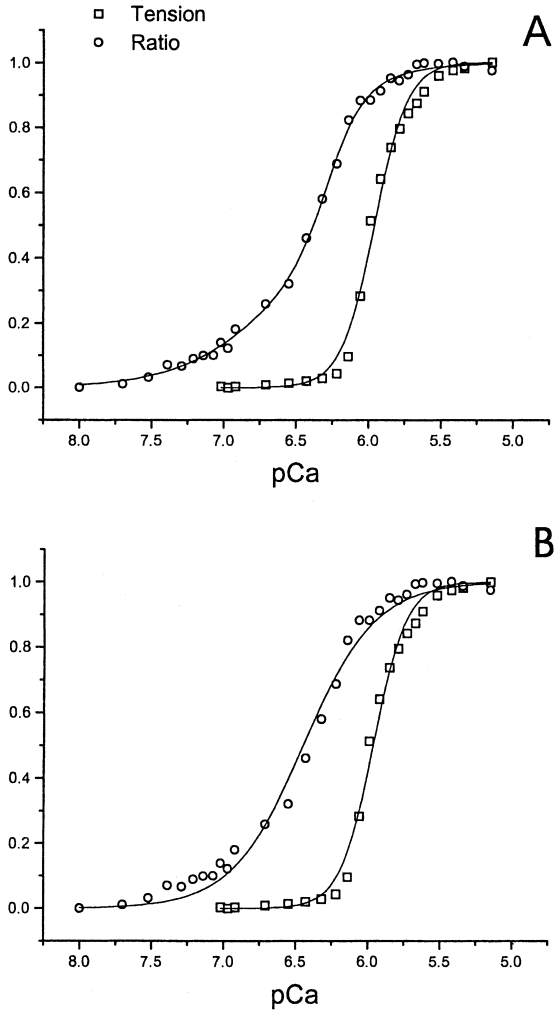

Fig. 6. (A) The pCa/ratio curve lies to the left of the pCa/force curve and saturates before the force saturates (Type I relationship). $pK_F = 5.96$ and $n_H = 3.8$, $P_o = 94$ mg, $pK_1 = 6.67$, $pK_2 = 6.28$, $n_1 = 1.3$, $n_2 = 3.7$, $A = 0.49$, and the $\chi^2 = 0.0003$. (B) The same force and ratio data as (A) but the ratio data are fit to a one binding site model, $pK_1 = 6.45$, $n_1 = 1.8$, and the $\chi^2 = 0.001$. Data collected in 0.1 mM Mg^{2+}.

Δ-fluorescence measures binding of Ca^{2+} to the low affinity sites of TnC and this initiates force. If the relative positions of the pCa/ratio and the pCa/force curves vary in a random way we would have to suspect that, even with our stringent criteria for accepting experiments as valid, the data are still contaminated with movement and other artifacts. There is a trend in the data, however, that is illustrated in Figure 7. The pCa/ratio curve synthesized from mean parameters for data collected in approximately the first 3 weeks after muscle harvest are to the right of that for data collected over the second three-week period. In contrast, the pCa/force curves for these intervals barely separate. There are about 50 experiments in each data pool. In both pools the sarcomere lengths vary and the fraction of TnC_{DANZ} inserted varies from 10 to 50%. The position of the pCa/ratio shifts from crossing the pCa/force curve (Type III) to being completely left of the force curve (Type I). By one month after muscle harvest, all the

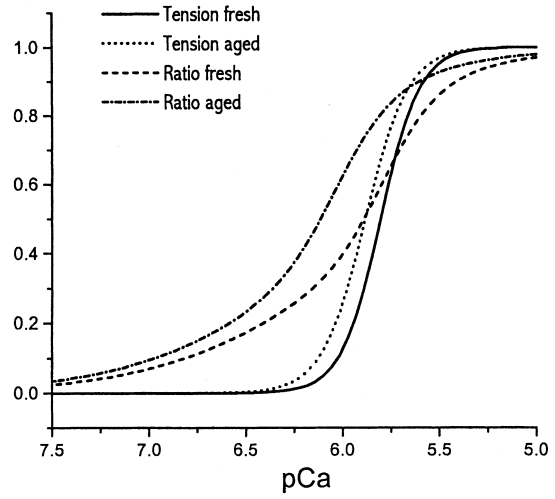

Fig. 7. This figure summarizes the effect of time after fiber harvest on the relative positions of the pCa/ratio and pCa/force curves. For fibers less than 3 weeks postharvest the mean ratio curve crosses over the force curve, however, as the fibers age the mean ratio curve shifts to the left. Curves drawn from the mean, best-fit parameters listed in Table 1.

pCa/ratio curves are left of the pCa/force curves (Types I and II). With sequential data collections on the same fiber, the pCa/ratio moves slightly to the left of the previous curve while the force curve is relatively stable (Table 1). The linear correlation between days postmuscle harvest and fitted parameters is listed in the lower half of Table 2. Extrapolation to zero-time postharvest predicts all curves will be type III at harvest. Plots of parameters derived from the relative position of the pCa/force and ratio curves against fiber stretch are listed in the upper half of Table 2. Some show no pattern or correlation with stretch (pK_1 and pK_2) while others (pK_F and n_H for example) do correlate with stretch.

Vanadate

To see if actively cycling cross-bridges affect the pCa/ratio curve some fibers were tested first in control then in

Table 1. Mean data for fresh (less than 3 weeks postharvest) and aged (beyond 3 weeks) skinned fibers

	Fresh	95% Conf.	Aged	95% Conf.
pK_1	6.215	0.058	6.371	0.045
n_1	2.35	0.44	2.7	0.52
pK_2	5.785	0.048	6.028	0.046
n_2	3.11	0.29	2.96	0.27
pK_F	5.80	0.026	5.88	0.034
n_H	4.3	0.28	3.9	0.17
Force	57.4	7.1	54.5	6.0
Number	51		57	

Mean data for fresh fibers cross over that for tension. After this period no individual cross over curves are seen. Force pK_F and n_H differ little between the two groups. Fibers were randomly stretched between 10 and 50% with an average of 27% for fresh and 29% for aged. The effects of stretch are listed in Table 2. Cross over incidence does not correlate with stretch. The table includes those tested in both low and high Mg^{2+}. Data plotted in Figure 7.

Table 2. Linear correlations for the pCa/force and pCa/ratio parameters with fiber stretch (upper eight rows) and with days postharvest (lower five rows)

	P-slope non-zero	Significance (%)	Slope	Intercept at 0 stretch	At 50% stretch
Correlation with percent stretch					
Force	0.002	>95	−0.6	85 mg	55 mg
pK_F	0.008	>95	0.003	5.75	5.9
n_H	0.0002	>95	−0.03	5.27	3.77
pK_1	0.06	<95	0.004	6.2	–
pK_2	0.1	<95	0.004	5.7	–
ΔF_G	0.005	>95	−0.8	78.4	38.4
ΔF_R	0.008	>95	−0.2	20.3	10.3
Correlation with days postharvest				Intercept at 0 days	
pK_F	<0.0001	>95	0.013	5.67	
n_H	0.039	<95	−0.04	4.93	
pK_1	<0.0001	>95	0.02	6.0	
PK_2	<0.0001	>95	0.03	5.4	

Stretch affects all but the pK_1 and pK_2 of the ratio. Days postharvest affect the p*K*s but not the n_H. The zero-day intercepts can be interpreted as the mean p*K*s at the time of muscle harvest, a cross-over condition where pK_2 is smaller than pK_F. There is no correlation between days postharvest and percent stretch. ΔF_G and ΔF_R are the fluorescence changes for the green and red channels respectively.

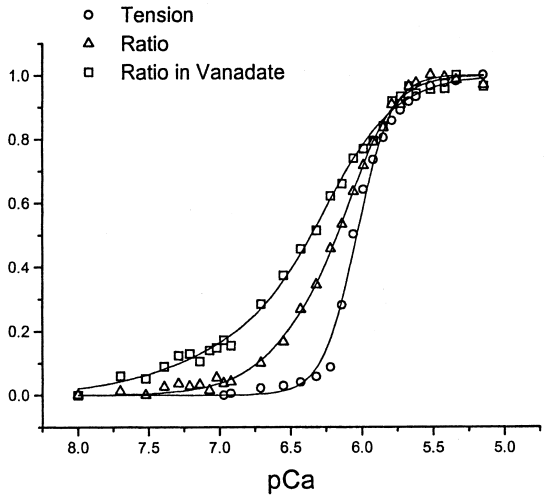

Fig. 8. Right most two curves are: control pCa/ratio and pCa/force curves. Left most curve is the pCa/ratio in the presence of 1 mM vanadate. In vanadate there is too little force to plot. Force $pK_F = 6.03$ and $n_H = 3.7$; Control $pK_1 = 6.42$, $pK_2 = 6.05$, $n_1 = 1.9$, $n_2 = 3.1$ $\chi^2 = 0.0006$. Vanadate $pK_1 = 6.95$, $pK_2 = 6.33$, $n_1 = 1.2$, $n_2 = 2.1$, $\chi^2 = 0.001$. Data summarized in Table 3.

Table 3. Fitting parameters for fibers tested in control saline (Contr.) are contrasted with those tested in 1 mM vanadate (Van.)

	Contr.	95% Conf.	Van.	95% Conf.
pK_1	6.38	0.056	7.1	0.54
n_1	1.0		1.0	
pK_2	5.05	0.064	6.61	0.51
n_2	3.05	0.276	2.8	0.52
Green baseline	201	6.9	195	6.6
ΔF_{green}	40	5.57	21	2.7
Red baseline	122	2.6	142	2.9
ΔF_{red}	1.5	0.43	2.4	0.36
pK_F	5.9	0.037	–	–
n_H	4.1	0.25	–	–
Force	67	5.88	2.5	0.53
Number	32		16	

Vanadate reduced the average force from 71 to 2.8 mg/fiber. pK_1 and pK_2 increase significantly over the controls but n_1 and n_2 do not. The green Δ-fluorescence in vanadate is about half the control. Most of the experiments are in saline containing high (1.0 mM) Mg^{2+}. Mean stretch of controls is 30% and of fibers bathed in vanadate 28%.

solutions containing 1 mM vanadate, an inhibitor of force generation (Solaro *et al.*, 1980), cross-bridge attachment (Kim *et al.*, 1998) and ATPase (Maughan *et al.*, 1995). Figure 8 shows control pCa/force and ratio curves and a second ratio curve subsequently collected in 1 mM vanadate. Vanadate shifts the ratio curve left. Vanadate treated fibers develop just a few milligrams of force so there is no corresponding pCa/force curve. The mean difference between pK_1 and pK_2 of the vanadate experiments (Table 3) is greater than 0.5 p-units. The mean left shift of the ratio curve with vanadate is greater than 0.4 p-units. The Δ-fluorescence of the green channel in vanadate is about half that of control fibers although vanadate has no apparent effect on total Ca^{2+} binding (Fuchs and Wang, 1991). The green baseline in vanadate is essentially the same as that in pCa 8 solution so there is no obvious effect of vanadate on TnC_{DANZ}. The smaller ratio change in vanadate at saturating [Ca^{2+}] is compatible with the argument that cycling cross-bridges enhance TnC_{DANZ} fluorescence but the left shift to higher [Ca^{2+}] sensitivity and lower cooperativity is not.

Discussion

pCa/force relative to pCa/ratio

A consistent, direct relationship between Ca^{2+} binding and muscle contraction is found in experiments that measure Ca^{2+} binding by isotope methods (Fuchs and Fox, 1982). However, when a fluorescent reporter of Ca^{2+} binding to TnC is substituted into skinned psoas fibers, a similar direct relation between the pCa/force and the pCa/Δ-fluorescence is not seen (Zot *et al.*, 1986; Guth and Potter 1987; Morano and Ruegg, 1991); the

pCa/Δ-fluorescence curve is displaced about 0.6 pCa units left of the pCa/force curve. It is suggested that cross-bridges may contribute to this displacement by pushing the regulatory units into a configuration that mimics the binding of Ca^{2+} (Guth and Potter, 1987; Morano and Ruegg, 1991). However, others report, the pCa/Δ-fluorescence relation is biphasic with the top half of the curve superimposing on force (Allen *et al.*, 1992). The pK of the upper half is 6.04, very close to that of the pCa/force curve. The authors suggest this represents binding to the low affinity, Ca^{2+} specific, regulatory sites of TnC. Based on a comparison of data in 1.0 and 0.05 mM Mg^{2+}, they also suggest that the lower half of the curve, a higher affinity site (pK_D 7.01), represents Ca^{2+} binding to the high affinity Ca^{2+}/Mg^{2+} structural sites. According to this interpretation the biphasic appearance of the pCa/Δ-fluorescence relationship reflects the two classes of divalent cation-binding sites in skeletal TnC (Potter and Gergely, 1975).

The present results confirm the biphasic property of the pCa/Δ-fluorescence relationship but also find the relative positions of the pCa/ratio and the pCa/force curves are variable. For the sake of discussion, we categorize this variability into three classes. In Type I the pCa/ratio is positioned completely left of the pCa/force curve (Guth and Potter, 1987; Morano and Ruegg, 1991). In type II the pCa/ratio curve partially superimposes on the upper half of the pCa/force curve (Allen *et al.*, 1992). In type III (current report) the ratio curve crosses over the pCa/force curve. The mean pK_1 is between 6.2 and 6.4, closer to pK_2 than the pK_2 (7.0) of Allen *et al.* (1992). The mean pK_2 of fresh muscle is about 5.8 (Table 1) and that of aged muscle is 6.03. The mean pK_1s in high (1 mM) and low Mg^{2+} (0.1 mM) are about the same (6.22 and 6.29 respectively). Thus, we find that the ratio curve is not very Mg^{2+} sensitive. Some of this discrepancy with Allen *et al.* (1992) could be due to differences in saline composition other than Mg^{2+} but this has not been explored.

The slope or n_H of the pCa/force curve may be key to explaining why, in half of the experiments on fresh fibers, the pCa/ratio crosses over the pCa/force curve (Figure 4). Although the mean pK_2 (5.8) for fresh fibers is essentially the same as the mean pK_F, in agreement with Allen *et al.* (1992), the mean n_H reported here is larger (4.3) than in previous reports (2–3) (Zot *et al.*, 1986 #1834; Guth and Potter, 1987 #1179; Allen *et al.*, 1992 #969). The pCa/ratio of type III curves might not cross-over the pCa/force curves if the n_H is low. This cannot be the only reason, however, because older fibers have similar high n_Hs and the ratio curves do not cross-over the force curves.

About 3 weeks after muscle harvest cross-over curves (type III) disappear and the pCa/ratio either partially superimposes on or is left of the relatively stable pCa/force curves (Figures 5, 6 and 7). With both fresh and older fibers repeated collections of pCa data tend to move the pCa/ratio curve further left but never enough to explain the loss of cross-overs in older fibers. Nor does sarcomere length seem to be a factor. It is unlikely that internal membrane systems capable of manipulating $[Ca^{2+}]$ are a factor because our Ca^{2+} buffer system is based on 10 mM EGTA and we are only recording steady state values. All the fibers in this study were randomly stretched between 10 and 50% and the type of pCa/ratio curve does not correlate with stretch, e.g. type III curves are seen at all degrees of stretch. The degree of replacement of native TnC with TnC_{DANZ} is not a factor because the fraction of TnC replaced (10–50%) does not correlate with curve type. The loss of type III curves with time postharvest is most likely due to subtle changes in protein–protein interactions but more studies are needed to isolate the cause.

TnC_{DANZ} in I-band vs. A-I-band

TnC extracts faster from the I than A-I-band (Yates *et al.*, 1993; Swartz *et al.*, 1997), therefore, more TnC_{DANZ} may end up in the I- than the A-I-band. If the type of ratio signal depends on the distribution TnC_{DANZ} between the two bands then the degree of stretch should affect the ratio in a systematic way. There is no correlation between the ratio type and fiber stretch. Nor does the ratio type depend on the percent TnC_{DANZ} in the fiber. TnC_{DANZ} is either not concentrated in the I-band or such concentration has little effect on the ratio. We also extracted all the TnC (TnC + TnC_{DANZ}) from the I-bands (rapidly extracting component – see below), of some labeled fibers, with no effect on the pCa/ratio data.

We showed previously that TnC extracts from skinned fibers in two components, a 'rapidly extracting component' (REC), complete in less than 15 s and equaling about 25% of the total, and a 'slowly extracting component' (SEC), half extracting in about 5 min (Brandt *et al.*, 1987). Removal of the REC has no effect on force or cooperativity and this was interpreted to mean that some TnC must be non-specifically bound. However, in light of reports that TnC in the I-band extracts faster that that in the A-I-band (Swartz *et al.*, 1997; Yates *et al.*, 1993), REC is most likely TnC from the I-band while the SEC is that from the A-I-band. This conclusion has implications for the mechanism of cooperative activation by Ca^{2+}.

Extraction of REC has no effect on tension or n_H while loss of SEC reduces both (Brandt *et al.*, 1984a,b, 1987). Because only loss of SEC (TnC from A-I-band) decreases n_H, cooperation between regulatory units must depend on the proximity of myosin. It is not solely a property of the thin filament. If the presence of myosin is essential for cooperation among regulatory units, the n_H should depend strongly on overlap, decreasing as overlap decreases. It does (Table 2). This argument also predicts that other interventions that limit or inhibit myosin cross-bridge contacts with the thin filament could reduce cooperation between regulatory units.

In the concerted transition formalism of allosteric systems adding an inhibitor increases cooperation while

introducing a second activator reduces it (Monod *et al*., 1965; Karlin, 1967; Brandt and Schachat, 1997; Brandt *et al*., 1987, 1990). One way myosin in the overlap zone could drive cooperative interactions between regulatory units is if weakly attached cross-bridges inhibit movement of the regulatory strand to the on position (for review see Reedy and Schachat, 1994). Extra Ca^{2+} would have to be bound to overcome this additional, myosin based, inhibition.

Judging by the pCa/ratio, in vanadate solutions Ca^{2+} affinity of TnC increases (Figure 8) and the n_H decreases. Vanadate forms the complex S1-ADP-Vanadate (Dantzig and Goldman, 1985; Chase *et al*., 1993); this is believed to move weakly attached cross-bridges closer to the myosin backbone (Takemori *et al*., 1995) and to inhibit strong binding of cross-bridges to the thin filament (Kim *et al*., 1998). Vanadate could, therefore, reduce the inhibition by weakly attached cross-bridges; this will lower the n_H and shift the pCa/ratio curve to the left as we observe (Figure 8 and Table 3). Vanadate may also inhibit other proposed cross-bridge mechanisms that are believed to augment activation of contraction (for review see Moss, 1992; Gordon *et al*., 2000).

The biphasic pCa/ratio signal

In all the pCa/ratio experiments reported here and those of Allen *et al*. (1992) fluorescence increase (pK_1) starts with the first increase in $[Ca^{2+}]$, almost one pCa unit higher than force threshold. Δ-Fluorescence increases with each stepwise increase in $[Ca^{2+}]$ until, at some point, there is a transition to a steeper rate of fluorescence increase (pK_2). With freshly harvested fibers this transition is at about the same pCa as the threshold of force. With older fibers the transition tends to precede force and be less cooperative. Thus, the coupling between the pCa/ratio and the pCa/tension curves is loose.

Most of the biphasic pCa/ratio curve can be directly related to the solution chemistry of TnC_{DANZ}. The pCa/Δ-fluorescence data from TnC_{DANZ} in solution are fit best with a model in which Ca^{2+} binding to either of the two low affinity, Ca^{2+} specific sites maximally enhance the fluorescence (Johnson *et al*., 1978). If that also applies to TnC_{DANZ} in skinned fibers, then pK_1 represents Ca^{2+} binding to either low affinity site on scattered TnCs. When sufficient Ca^{2+} is bound to overcome the sum of all inhibitory factors, an abrupt change in the conformation (position) of the regulatory strand promotes contraction and additional Ca^{2+} binding. Some of the TnCs have two empty low affinity sites hence the additional increase in fluorescence. In support of this proposed mechanism, the mean n_1 is 1.3, close to expectation for non-cooperative binding to either site, and n_2 is 3.0, in keeping with a cooperative switch mechanism (data for all 106 fibers fit with the two site model and five free parameters). As postharvest time increases, inhibition of the Ca^{2+} trigger mechanism weakens and the fraction of binding sites on TnC_{DANZ} that must be occupied to initiate the conformational transition is reduced. In older fibers, the start of the second fluorescence increase (pK_2) shifts left on the pCa axis (Figures 6 and 7).

pK_1 is unlikely to represent Ca^{2+} binding to the high affinity sites on TnC. In solution the two classes of sites on TnC are separated by about two pCa units (Potter and Gergely, 1975), one pCa unit more than that found by Allen *et al*. (1992) and 1.5 pCa units more than that reported here. Also in solution Ca^{2+} or Mg^{2+} binding to the high affinity sites reduces, not increases, the fluorescence of TnC_{DANZ} by 17 and 21% respectively (Johnson *et al*., 1978). For fibers bathed 1 mM Mg^{2+} saline a 4% increase in fluorescence is the maximum expected and this can only occur if Ca^{2+} displaces Mg^{2+} from the high affinity sites. For fibers bathed in 0.1 mM Mg^{2+} saline, Ca^{2+} occupation of empty high affinity sites should decrease fluorescence. Neither of these conditions predicts the relatively large increase in fluorescence described by pK_1.

We argue that, in skinned fibers, the pCa/ratio curve need not bear a constant relation to the pCa/force and that variability, in this relationship, is not simply a question of experimental techniques. The tendency of the pCa/ratio curve to move left with fiber age and condition may, in part, explain why the pCa/Δ-fluorescence curves of some reports (Guth and Potter, 1987; Zot and Potter, 1987; Morano and Ruegg, 1991) are left of the pCa/force curve while those of others overlap it (Allen *et al*., 1992). By studying a very large number of fibers in a wide range of conditions, we have reproduced the results of previous groups. In addition, we find that in very fresh fibers the pK_2 component of the pCa/ratio curve often crosses over the pCa/force curve. Loose coupling between the initial Ca^{2+} binding and the cooperative switch point may account for much of the variation in the shape and position of the pCa/ratio relative to the pCa/force curve.

Acknowledgements

Supported by grants from NIH: AR40300 (PWB), EY11377 (FHS), and HL51885 (DB).

References

Allen TS, Yates LD and Gordon AM (1992) Ca(2+)-dependence of structural changes in troponin-C in demembranated fibers of rabbit psoas muscle. *Biophys J* **61(2):** 399–409.

Brandt PW and Schachat FH (1997) Troponin C modulates the activation of thin filaments by rigor cross-bridges. *Biophys J* **72(5):** 2262–2267.

Brandt PW, Reuben JP and Grundfest H (1972) Regulation of tension in the skinned crayfish muscle fiber. II. Role of calcium. *J Gen Physiol* **59(3):** 305–317.

Brandt PW, Cox RN and Kawai M (1980) Can the binding of Ca^{2+} to two regulatory sites on troponin-C determine the steep pCa/tension relationship of skeletal muscle? *Proc Natl Acad Sci USA* **77:** 4717–4720.

Brandt PW, Diamond MS, Gluck B, Kawai M and Schachat F (1984a) Molecular basis of cooperativity in vertebrate muscle thin filaments. *Carlsberg Res Commun* **49:** 155–167.

Brandt PW, Diamond MS and Schachat FH (1984b) The thin filament of vertebrate skeletal muscle co-operatively activates as a unit. *J Mol Biol* **180(2):** 379–384.

Brandt PW, Diamond MS, Rutchik JS and Schachat FH (1987) Co-operative interactions between troponin–tropomyosin units extend the length of the thin filament in skeletal muscle. *J Mol Biol* **195(4):** 885–896.

Brandt PW, Roemer D and Schachat FH (1990) Co-operative activation of skeletal muscle thin filaments by rigor cross-bridges. The effect of troponin C extraction. *J Mol Biol* **212(3):** 473–480.

Chase PB, Martyn DA, Kushmerick MJ and Gordon AM (1993) Effects of inorganic phosphate analogues on stiffness and unloaded shortening of skinned muscle fibres from rabbit. *J Physiol* **460:** 231–246.

Dantzig JA and Goldman YE (1985) Suppression of muscle contraction by vanadate. Mechanical and ligand binding studies on glycerol-extracted rabbit fibers. *J Gen Physiol* **86(3):** 305–327.

Eastwood AB, Wood DS, Bock KL and Sorenson MM (1979) Chemically skinned mammalian skeletal muscle. I. The structure of skinned rabbit psoas. *Tissue & Cell* **11:** 553–566.

Ebashi S, Endo M and Ohtsuki I (1969) Control of muscle contraction. *Rev Biophys* **2:** 351–384.

Fraser ID and Marston SB (1995) *In vitro* motility analysis of actin–tropomyosin regulation by troponin and calcium. The thin filament is switched as a single cooperative unit. *J Biol Chem* **270(14):** 7836–7841.

Fuchs F (1977) The binding of calcium to glycerinated muscle fibers in rigor. *Biochem. Biophys Acta* **491:** 523–531.

Fuchs F (1985) The binding of calcium to detergent-extracted rabbit psoas muscle fibres during relaxation and force generation. *J Muscle Res Cell Motil* **6(4):** 477–486.

Fuchs F and Fox C (1982) Parallel measurements of bound calcium and force in glycerinated rabbit psoas muscle fibers. *Biochim Biophys Acta* **679(1):** 110–115.

Fuchs F and Wang YP (1991) Force, length, and Ca(2+)-troponin C affinity in skeletal muscle. *Am J Physiol* **261(5 Pt 1):** C787–C792.

Gordon AM, Homsher E and Regnier M (2000) Regulation of contraction in striated muscle. *Physiol Rev* **80(2):** 853–924.

Guth K and Potter JD (1987) Effect of rigor and cycling cross-bridges on the structure of troponin C and on the Ca^{2+} affinity of the Ca^{2+}-specific regulatory sites in skinned rabbit psoas fibers. *J Biol Chem* **262(28):** 13,627–13,635.

Johnson JD, Collins JH and Potter J (1978) Dansylaziridine-labeled troponin C: a fluorescent probe of Ca^{2+} binding to the Ca^{2+}-specific regulatory sites. *J Biol Chem* **253(18):** 6451–6458.

Karlin A (1967) On the application of 'a plausible model' of allosteric proteins to the receptor for acetylcholine. *J Theor Biol* **16(2):** 306–320.

Kim DS, Takezawa Y, Ogino M, Kobayashi T, Arata T and Wakabayashi K (1998) X-ray diffraction studies on the structural changes of rigor muscles induced by binding of phosphate analogs in the presence of MgADP. *Biophys Chem* **74(1):** 71–82.

Martyn DA, Freitag CJ, Chase PB and Gordon AM (1999) Ca^{2+} and cross-bridge-induced changes in troponin C in skinned skeletal muscle fibers: effects of force inhibition. *Biophys J* **76(3):** 1480–1493.

Maughan DW, Molloy JE, Brotto MA and Godt RE (1995) Approximating the isometric force-calcium relation of intact frog muscle using skinned fibers. *Biophys J* **69(4):** 1484–1490.

Monod J, Wyman J and Changeux JP (1965) On the nature of allosteric transitions: a plausable model. *J Mole Biol* **12:** 88–118.

Morano I and Ruegg JC (1991) What does TnCDANZ fluorescence reveal about the thin filament state? *Pflug Arch* **418(4):** 333–337.

Moss RL (1992) Ca^{2+} regulation of mechanical properties of striated muscle. Mechanistic studies using extraction and replacement of regulatory proteins. *Circ Res* **70(5):** 865–884.

Moss RL, Giulian GG and Greaser ML (1985) The effects of partial extraction of TnC upon the tension-pCa relationship in rabbit skinned skeletal muscle fibers. *J Gen Physiol* **86(4):** 585–600.

Moss RL, Swinford AE and Greaser ML (1983) Alterations in the Ca^{2+} sensitivity of tension development by single skeletal muscle fibers at stretched lengths. *Biophys J* **43(1):** 115–119.

Potter JD and Gergely J (1975) The calcium and magnesium binding sites on troponin and their role in the regulation of myofibrillar adenosine triphosphatase. *J Biol Chem* **250(12):** 4628–4633.

Reedy MK and Schachat F (1994) Does Resolution Lead to Reconcilliation? New electron microscopic data provide direct evidence in support of the classic steric-blocking model for regulation of actin–myosin interactions by tropomyosin. *Curr Biol* **4:** 624–626.

Solaro RJ, Holroyde MJ, Wang T, Matlib MA, Grupp I and Grupp G (1980) Effects of vanadate on biochemical and contractile properties of rabbit hearts. *J Cardiovasc Pharmacol* **2(4):** 445–452.

Swartz DR, Moss RL and Greaser ML (1997) Characteristics of troponin C binding to the myofibrillar thin filament: extraction of troponin C is not random along the length of the thin filament. *Biophys J* **73(1):** 293–305.

Takemori S, Yamaguchi M and Yagi N (1995) An X-ray diffraction study on a single frog skinned muscle fiber in the presence of vanadate. *J Biochem (Tokyo)* **117(3):** 603–608.

Weber A and Winicur S (1961) The role of calcium in the superprecipitation of actomyosin. *J Biol Chem* **236:** 3198–3202.

Wood DS, Zollman J, Reuben JP and Brandt PW (1975) Human skeletal muscle: properties of the 'chemically skinned' fiber. *Science* **187:** 1075–1076.

Yates LD, Coby RL, Luo Z and Gordon AM (1993) Filament overlap affects TnC extraction from skinned muscle fibres. *J Muscle Res Cell Motil* **14(4):** 392–400.

Zot HG and Potter JD (1982) A structural role for the Ca^{2+}–Mg^{2+} sites on troponin-C in the regulation of muscle-contraction – preparation and properties of troponin-C depleted myofibrils. *J Biol Chem* **257(13):** 7678–7683.

Zot HG and Potter JD (1987) Calcium binding and fluorescence measurements of dansylaziridine-labelled troponin C in reconstituted thin filaments. *J Muscle Res Cell Motil* **8(5):** 428–436.

Zot HG, Guth K and Potter JD (1986) Fast skeletal muscle skinned fibers and myofibrils reconstuted with N-terminal fluorescent analogues of troponin C. *J Biol Chem* **261:** 15,883–15,890.